Revisiting Indocyanine Green: Effects of Serum and Physiological Temperature on Absorption and Fluorescence Characteristics

Bongsu Jung, Valentine I. Vullev, and Bahman Anvari

***Abstract*—Indocyanine green (ICG) remains as the only near infrared dye approved by the FDA. Despite its long history of usage in clinical medicine, a systematic study of the effects of serum proteins at physiologically relevant levels and temperature on absorption and fluorescence characteristics of ICG has been missing. We incubated ICG at concentrations in the range of 0.6–25.8 μM in McCoy's 5a cell culture medium, without and with supplemental fetal bovine serum (FBS) at 5% and 10% levels. Our analyses of absorption and fluorescence spectra indicate that the peak absorbance of ICG associated with its monomeric form increases in the presence of FBS. For example, at ICG concentration of 25.8 μM, the monomer absorbance is increased by nearly 100% in the presence of 10% FBS. Similarly, there is an increase in the relative fluorescence quantum yield of ICG, by as much as nearly 3.5 times in the presence of FBS. When incubated at 37 °C, the presence of FBS in the cell culture medium helps maintain the monomeric absorption of ICG and sustain the increased fluorescence emission. We offer explanations to describe the possible photophysical mechanisms underlying the observed effects and discuss the importance of these results to *in-vivo* applications of ICG.**

***Index Terms*—Albumin, blood, dye, lasers, lymphography, near infrared, ophthalmic angiography, optical imaging, photodynamic therapy, photothermal therapy, phototherapy, sentinel lymph nodes.**

I. Introduction

INDOCYANINE green (ICG) is a water-soluble tricarbocyanine dye that absorbs in the near infrared (NIR) spectral band. The first reports for medical applications of ICG date back to the late 1950s to measure cardiac output [1]. The finding that ICG is almost exclusively uptaken by the liver, led to its application in assessment of hepatic function [2]. ICG received supplemental approval by United Stated Food and Drug Administration (FDA) for ophthalmic angiography in 1975. To date, ICG remains the only FDA-approved NIR dye for cardiocirculatory measurements, liver function tests, and ophthalmological imaging, predominantly involving choroidal circulation [3], [4]. ICG has also been investigated for sentinel lymph node (SLN) mapping and staging in cancer patients [5]–[13], in lymphography to assess lower and upper lymphedema [14]–[17], in lymphangiogenesis analysis following treatment of lymphedema by tissue replantation [18], and in assessment of anastomatic perfusion [19], [20]. Polom *et al.* provide an excellent and further review of the utility of ICG-guided imaging for SLN detection, lymphedema evaluation, and assessment of microvascular circulation of free flaps in reconstructive surgery [21]. Additionally, ICG has been investigated for potential therapeutic applications such as photodynamic therapy (PDT) [22]–[24], tissue welding [25], and photothermal treatment of skin diseases [26], [27].

FOR *in-vivo* applications, ICG is administered by intravascular injection. While blood plasma contains an array of proteins, it is known that ICG mainly binds to albumin and alpha-1 lipoprotein [28]–[34]. Specifically, it is reported that 95% and 4% of ICG bind to albumin and alpha globulin proteins in blood, respectively [28]. When dissolved in aqueous solution, ICG exhibits maximum absorbance at 790 nm, corresponding to the peak absorption of its monomeric form. However, when in a solution containing 5% serum albumin, its spectral peak shifts to 815 nm, which suggests the presence of ICG in a composite form [28]. It has been reported that the absorbance of ICG ($\approx$ 1.6 mM) at its spectral peak is reduced by 10% after 10 h of storage in water and direct light [35]. However, when ICG was dissolved in Ringer's solution containing 2% and 4% human serum albumin (HSA), its peak spectral absorption was reduced by less than 2% following 10 h of storage in direct light [35]. It has also been reported that at a fixed ICG concentration ($\approx$ 6.4 mM) in Ringer's solution, the value of its maximal absorbance increases by approximately twofold in presence of 2% and 4% HSA and direct light as compared to the solution without HSA [35]. Similarly, the peak absorbance of 6.4 mM ICG in fresh pig and human plasma was $\approx$ 10% higher than that of ICG in water and direct light [35]. In addition to the effects of albumin on ICG absorption, other investigators have reported that the natural degradation kinetics of ICG at room temperature is reduced in the presence of HSA [36].

Fluorescence emission characteristics of ICG have also been reported to vary as a result of binding to serum proteins. When dissolved in phosphate buffer solution containing 50 g/l HSA, the fluorescence quantum yield of ICG has been reported to remain almost constant over the concentration range of $\approx$ 1.1–110 μM. However, when dissolved in water, its fluorescence

Manuscript received June 2, 2013; revised August 10, 2013; accepted August 12, 2013. Date of publication August 15, 2013; date of current version October 25, 2013. This work was supported in part by the National Science Foundation under Grant CBET-1144237 and Grant CBET-0923408.

B. Jung was with the Department of Bioengineering, University of California, Riverside, CA 92507 USA. He is now with Daegu-Gyeongbuk Medical Innovation Foundation, Daegu, Korea (e-mail: bsjung@dgmif.re.kr).

V. I. Vullev and B. Anvari are with the Department of Bioengineering, University of California, Riverside, CA 92521 USA (e-mail: vulev@ucr.edu; anvarib@ucr.edu).

Color versions of one or more of the figures in this paper are available online at http://ieeexplore.ieee.org.

Digital Object Identifier 10.1109/JSTQE.2013.2278674

quantum yield decreased by approximately two orders of magnitude over the same concentration range [37].

Although changes in optical properties of ICG have been observed in the presence of albumin, previous studies have been limited to either a fixed HSA level [28], [37], or have not investigated the fluorescence characteristics of ICG over a broad range of ICG concentration in presence of serum proteins [35], [36]. To fill this void, we present a systematic study of the effects of serum at physiological levels and temperature on the absorption and fluorescence characteristics of ICG in the range of 0.6–25.8 μM. We simulated the physiological environment of ICG by incubating it in McCoy's 5a cell culture medium supplemented with Fetal Bovine Serum (FBS) and analyzed the resulting absorption and fluorescence spectra. We also investigated the role of serum in preventing the thermal degradation of ICG. We offer descriptions of possible photophysical mechanisms for the observed effects and discuss the relevance of our findings to practical *in-vivo* applications of ICG.

II. Methods and Materials

A. Materials

McCoy's 5A cell culture medium, which contains various inorganic salts (predominantly KCl, NaCl, and Na_2HPO_4), amino acids (predominantly L-glutamine), vitamins, and other macromolecules (predominantly D-glucose) was purchased from ATCC (30-2007, Manassa, VA, USA). FBS was purchased from Invitrogen (Grand Island, NY, USA). Bovine serum albumin (BSA) has highest relative concentration among the proteins in FBS [38]–[40]. ICG powder (Sigma-Aldrich) was used as received. Various FBS concentrations (5% and 10%, v/v) were prepared to supplement the McCoy's 5A culture medium. We initially prepared a stock solution of ICG (650 μM) in deionized (DI) water, and subsequently, diluted it to various levels (0.6 μM$-$25.8 μM) in the presence of the cell culture medium. Considering that the reported ICG dosages in procedures such as SLN biopsy include values in the range of $\approx$ 7.8 μg/ml–12.5 mg/ml ($\approx$ 10 μM–16 mM) [21], giving effective dosages of 0.017–27 μM (based on dilution factor of $\approx$ 600 following injection), the ICG concentrations used in this study (0.6–25.8 μM) are clinically relevant, and comparable to those used in some of the clinical applications.

B. Absorption and Fluorescence Spectroscopy, and Calculation of Relative Fluorescence Quantum Yield

Absorption spectra of various samples at room temperate were obtained in the 230–900-nm spectral range using a UV-Visible-Near IR (UV-Vis-NIR) spectrometer (Cary 50, Varian Inc.). We used a Xenon arc lamp in conjunction with a monochromator to provide filtered light at either 650 or 750 nm to photoexcite the samples. NIR Fluorescence emission spectra (665–900 nm) from the samples were obtained by a fluorescence spectrophotometer (Fluorolog, Horiba-Jobin-Yvon, Inc.). We used a cuvette with 10-mm light path for absorption and fluorescence measurements.

We calculated the wavelength (λ)-dependent normalized fluorescence spectra ($\chi(\lambda, C)$) at a given excitation wavelength ($\lambda_{\rm ex}$) and ICG concentration (C) as

$$\chi(\lambda, C) = F(\lambda, C)/(1 - 10^{-A(\lambda_{\rm ex}, C)}) \tag{1}$$

where $F(\lambda, C)$ is emitted fluorescence intensity, and A is the absorbance value at $\lambda_{\rm ex}$ for a given ICG concentration. The normalized integrated fluorescence intensity (ρ), which is a measure of the fluorescence quantum yield, was calculated as

$$\rho(C) = \int F(\lambda) d\lambda/(1 - 10^{-A(\lambda_{\rm ex}, C)}). \tag{2}$$

To determine the *relative* fluorescence quantum yield (ϕ) at a given ICG concentration, we proceeded as follows: first, we fitted the profiles of ρ as a function of ICG concentration in the range of 0.6–19.4 μM with a single exponentially decaying function. We then extrapolated the exponential function to a very dilute ICG concentration (C_0) (near zero on the ordinate) and estimated the parameter ρ at C_0. Finally, we determined ϕ(C) as

$$\phi(C) = \rho(C)/\rho(C_0). \tag{3}$$

C. Influence of Serum Proteins and FBS on the Absorption and Fluorescence of ICG

McCoy's 5A cell culture media supplemented with different levels of FBS (0%, 5%, and 10% v/v) were prepared. Various ICG concentrations were added to the cell culture media. Subsequently, we obtained the absorption and fluorescence spectra of the various solutions in dark at room temperature. We assigned 778 and 791 nm, corresponding to the peak absorption wavelength by the monomeric forms of ICG in the absence or presence of FBS, respectively, as the reference wavelengths in our characterization analyses.

D. Influence of Physiological Temperature on ICG Absorption in the Presence of FBS

A temperature-controlled water bath at 37 °C [Thermo Fisher Scientific (Fairlawn, NJ, USA)] was used to incubate the samples containing 13 μM of ICG dissolved in the cell culture medium with various levels of supplemental FBS (0%, 5%, 10% v/v). The incubations times were 1, 2, 3, and 17 h. Immediately after each incubation time, we obtained the absorption and fluorescence spectra in response to 750-nm photoexcitation of the samples. The monomeric absorption peaks (778 nm for FBS 0% and 791 nm for FBS 5% and 10%) at each sample were chosen to analyze the effects of FBS on thermal stability of ICG.

III. Results and Discussion

When dissolved in DI water as the control solvent, ICG exhibited absorption with a maximum at 780 nm that was the dominant feature over the entire investigated concentration range, i.e., 0.6–13 μM [see Fig. 1(a)]. As the concentrations exceeded 2.6 μM, a second peak at approximately 714 nm appeared [see Fig. 1(a)].

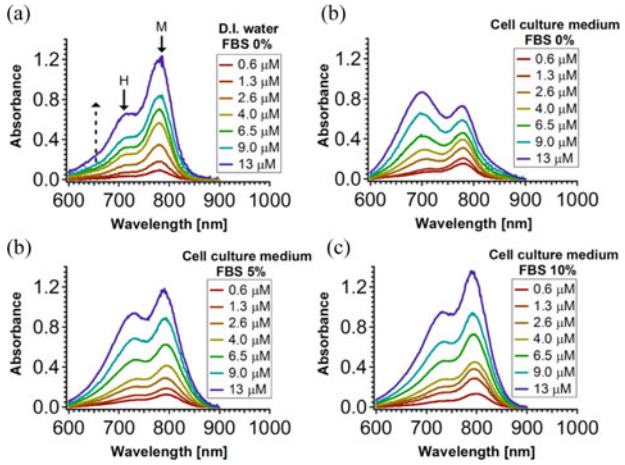

Fig. 1. Absorption spectra of ICG in (a) DI water with FBS 0% as control, and McCoy's 5A medium supplemented with (b) FBS 0%, (c) FBS 5%, and (d) FBS 10%. Numbers in the legend are the ICG concentration in μM. Dashed arrow indicates the direction of ICG concentration increase. H-like aggregation and Monomer forms of ICG are designated as H and M, respectively.

We ascribe the peaks at 780 and 714 nm to the monomeric and aggregated forms of ICG, respectively [37].

When dissolved in McCoy's 5A cell culture medium without FBS the absorption peak of the ICG monomeric form appeared at 778 and was dominant at ICG concentrations < 6.5 μM [see Fig. 1(b)]. However, with an increase in ICG concentration above 6.5 μM, the presence of a second peak at approximately 700 nm became progressively more dominant [see Fig. 1(b)]. Similar to the observed concentration-dependent spectral features for aqueous media, we attribute the origin of this secondary peak to aggregation of ICG (i.e., to the formation of H-like aggregates) [37], [41]. We use the term "H-like aggregate" since our data are based on spectral information, rather than high-resolution structural information.

The addition of FBS to the cell culture media caused a bathochromic (red) shift of the monomeric absorption peak of ICG to 791 nm [see Fig 1(c) and (d)]. Monomer absorption remained dominant over the entire range of ICG concentration (0.6–13 μM) in the presence of FBS [see Fig. 1(c) and (d)], and its absorbance (A) value increased as compared to those in the absence of FBS [see Fig. 1(b)]. Furthermore, the H-like aggregate absorption peak at 700 nm in the absence of FBS [see Fig. 1(b)] was bathochromically shifted to 730 nm for all ICG concentrations examined (0.6–13 μM) in the presence of FBS [see Fig. 1(c) and (d)]. The A values associated with the H-like aggregate forms remained consistently lower than those of the monomeric form [see Fig. 1(c) and (d)]. Our observed bathochromic shifts in ICG absorption spectra in the presence of FBS are consistent with those reports by other investigators [28], [37], [42]. When increasing the ICG concentration level from 0.6 to 13 μM, there were 5- and 8-nm hypsochromic (blue) shifts in the monomer absorption peaks in the presence of FBS at 5% and 10% levels, respectively [see Fig. 1(c), and (d)].

We attribute the FBS-induced changes in ICG spectral properties to the BSA constituent in FBS. BSA has the highest

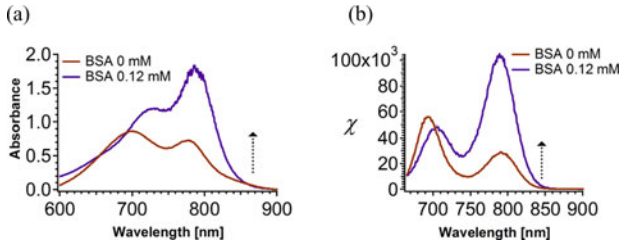

Fig. 2. (a) Absorption and (b) normalized fluorescence spectra (χ) of ICG in McCoy's 5A cell culture medium without and with BSA (0.12 mM). ICG concentration was 13 μM. Dotted arrow indicates the direction of BSA level increase.

relative concentration among the proteins in FBS [38]–[40]. To test our hypothesis, we added BSA (0.12 mM) to the McCoy's 5A cell culture medium without FBS. Spectral recording made immediately after introducing BSA into the cell culture medium revealed that the absorption and fluorescence peaks associated with the monomeric form of ICG (13 μM) were enhanced (see Fig. 2). Additionally, there was a bathochromic shift in the monomer absorption peak from 778 to 787 nm upon addition of 0.12-mM BSA to the medium. If we consider the 700 nm as the absorption peak of the H-like aggregate form of ICG in the absence of BSA, there was a bathochromic shift to 724 nm in the presence of 0.12-mM BSA. Similarly, there was a bathochromic shift in the fluorescence emission associated with the H-like aggregate from 693 nm in the absence of BSA to 705 nm in the presence of 0.12-mM BSA. However, there was no significant bathochromic shift (less than 1 nm) in the fluorescence emission of monomeric ICG at 790 nm.

The exciton theory for molecular spectroscopy provides an explanation for the origin of the observed spectral features [43], [44]. Aggregation-induced split in the energy levels of the excited state results from two orthogonal types of molecular arrangements: J- and H-aggregates. J-aggregates involve a linear "head-to-tail" arrangement of the transition dipole moments of the chromophores, whereas H-aggregates adopt geometries in which the individual chromophores, and their transition dipoles, are arranged in a stacked (sandwich-like) manner [43], [45]–[47]. The excitonic coupling between the chromophores in the J- and H-aggregates splits their excited states into two new nondegenerate states, i.e., two states with different energy levels. In the J-aggregates, the excitonically formed state with lower energy involves codirectionally oriented transition dipole moments, while the upper-level excitonic state comprises transition dipoles with opposite orientations. Conversely, in H-aggregates, the codirectional arrangement of the transition dipoles raises the excited-state energy (forming the upper-level excitonic state), while oppositely oriented transition dipoles lower the excited-state energy (resulting in the lower-level state).

Should the vector sum of the transition dipole moments of aggregated chromophores be zero (i.e., when the dipoles have opposing orientations), the electronic transition is forbidden and cannot be spectrally observed. Therefore, for J-aggregates, only the transitions to the lower level of the split-excited state are allowed, causing a red spectral shift. Conversely, for H-aggregates,

transitions to only the upper energy level of the excited state are allowed, resulting in a blue spectral shift. Therefore, we associate the hypsochromic shifts to the secondary peaks [see Fig. 1(b)] with the H-like aggregates of ICG.

Self-assembly of ICG depends on its concentration, pH, temperature, ionic strength, and polarity of the solvent [43], [47]. Among these factors, increased ionic strength of the media increases the amount of dye H-like aggregates [43], [45], [47], [48]. That is, the increased ion concentration provides an effective screening of the positive charge delocalized on the cyanine chromophore, allowing hydrophobically driven self-assembly via π–π stacking, leading to H-like aggregation. The McCoy's 5A cell culture medium has a higher ionic strength (0.130 mol/l) than DI water, which we attributed to the presence of H-like aggregates at ICG concentration greater than 6.5 μM [see Fig. 1(a) and (b)].

Extending the exciton theory to assemblies with oblique arrangement of the transition dipoles offers an explanation for the observed spectral shifts of the H-like aggregate of ICG, induced by the presence of FBS and BSA. H- and J-aggregates are the two extreme types of orthogonal geometry that cause blue and red spectral shifts. In reality, it is likely for the dyes to assemble in an oblique manner, hence forming aggregates with transition dipoles that are not oriented in parallel. Depending on the excitonic coupling among the ICG molecules as well as the angles between the transition dipoles, such oblique aggregates can manifest spectral blue shifts, red shifts, or both. Such spectral shifts are quite sensitive to changes in the arrangement of the dye molecules in an aggregate. Components of the cell culture media and of FBS bind ICG, providing templates for formation of aggregates arrangement that differ from the arrangement of the aggregates formed spontaneously in the DI water environment.

We quantified the effects of various FBS levels on ICG monomeric absorption [see Fig. 3(a)]. At ICG concentrations of 3.87 μM, there were approximately 4% and 13% increases in the monomer absorbance (A_{monomer}) when the FBS level increased from 0% to 5% and 10% levels, respectively. This difference became progressively larger to much as 75% and 100% in the presence of 5% and 10% FBS, respectively, with increased ICG concentration at 25.8 μM. When the FBS level was increased from 5% to 10%, A_{monomer} increased by 8% to 26% over the ICG concentration range examined.

We define $\psi = A_{\mathrm{monomer}}/A_{\mathrm{H\text{-}like\,aggregate}}$, where $A_{\mathrm{H\text{-}like\,aggregate}}$ corresponds to values of H-like aggregate absorbance levels. In the presence of 5% FBS, value of ψ increased by 10–76% for ICG concentrations in the range of 3–13 μM [see Fig. 3(b)]. In the presence of 10% FBS, value of ψ increased by 50–110% for ICG concentrations in the range of 3–13 μM [see Fig. 3(b)]. These findings can be explained on the basis that some of the ICG molecules introduced into the cell culture medium can bind to BSA as monomers, resulting in reduced amounts of ICG available for self-aggregation. Increased levels of ICG monomers combined with decreased levels of H-like aggregates give rise to higher ψ in the presence of FBS.

BSA has similar molecular structure to HSA except that it has two tryptophan residues, whereas HSA has only one

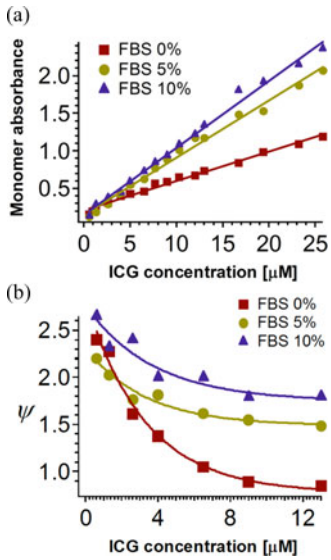

Fig. 3. (a) Absorbance values corresponding to the monomeric form of ICG at different concentrations. Measurements were obtained using ICG dissolved in McCoy's 5A without and with supplemental FBS. Lines are fits to the experimental data. (b) Effect of FBS on parameter ψ, defined as the ratio of $A_{\mathrm{monomer}}/A_{\mathrm{H\text{-}like\,aggregate}}$ of ICG molecules in McCoy's 5A cell culture medium. Curves are monotonically decaying single exponential fits to the experimental data.

tryptophan [49], [50]. Therefore, we can expect that the interaction between ICG and BSA would be similar to those between HSA and ICG. It is reported that 1–2 ICG molecules bind mainly to the hydrophobic core of HSA [31], [32], [34], [51]. Therefore, when ICG molecules were introduced into the McCoy's 5A cell culture medium containing FBS, they bound to BSA as monomers at their assigned binding sites. This binding results in increased values of A_{monomer} [see Fig. 3(a)]. The excess nonbound ICG molecules self-aggregated, manifesting the characteristic H-like aggregate absorption peak [see Fig. 1(c) and (d)].

Our observation of enhanced monomeric absorbance of ICG in the presence of FBS [see Fig. 3(a)] is consistent with a previous study in which the absorbance associated with monomeric form of the dye, bis(heptamethine cyanine), increased with higher levels of HSA [47]. Similarly, in another study, the monomeric absorbance of cypate, a NIR dye with a structural analogy to ICG, was enhanced in presence of BSA [52].

Dye aggregation can be reduced by increasing the hydrophobicity of the solvent [47], [48]. Since dilute aqueous solutions of alcohols are hydrophobic systems [53], increasing the alcohol content of a solvent will result in increased hydrophobicity. For example, Beckford *et al*. have reported that the ratio of monomer to aggregate peak absorbance of Benz[c,d]indolium, Benz[e]indolium and Fischer indolium cyanine dyes increased with increasing levels of the solvent hydrophobicity as modulated by changing the ratio of methanol to buffer [48]. Similarly, Patonay *et al*. have reported that monomer absorbance of bis(heptamethine cyanine) dye 7 increases approximately by factor of 7 when the solvent is changed from 1% to 100% methanol [47]. Furthermore, these latter investigators observed that the monomer absorbance increased by nearly a factor of

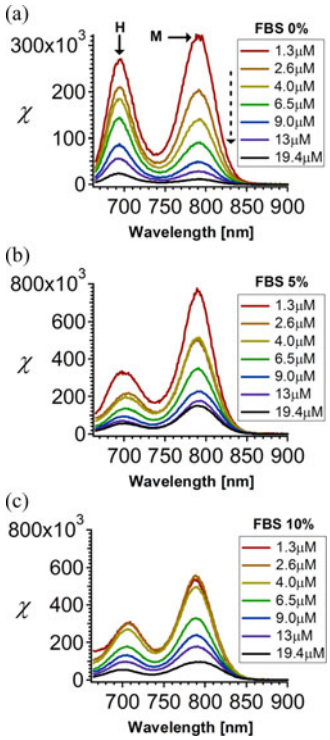

Fig. 4. Normalized fluorescence spectra (χ) of ICG in McCoy's 5A cell medium with (a) 0%, (b) 5%, and (c) 10% FBS. The legends indicate ICG concentrations. The excitation wavelength was 650 nm. Dashed arrow indicates the direction of ICG concentration increase.

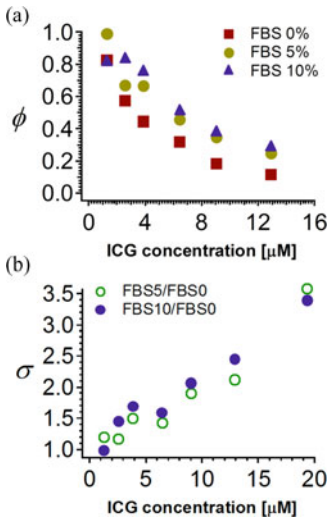

Fig. 5. (a) Relative fluorescence quantum yield (ϕ) of ICG in McCoy's 5A cell culture medium with and without FBS as a function of ICG concentrations, and (b) ratio of $\phi_{\text{with FBS}}/\phi_{\text{without FBS}}$ (defined as σ). Excitation wavelength was 750 nm.

2.5 in the presence of HSA ranging between 0 and 100 μM. This observation was explained on the basis that when bound to HSA, the dye is in a more hydrophobic environment than aqueous buffer. In a similar manner, when bound to BSA, the local environment of ICG may be more hydrophobic than that of the cell culture medium without supplemental FBS. This enhanced hydrophobic environment could be another contributing factor in reducing self-aggregation of ICG and, subsequently, increasing its monomeric absorbance.

We present the influence of FBS on fluorescence emission of ICG in McCoy's 5A cell culture medium (see Fig. 4). In response to 650-nm excitation, the fluorescence spectra of ICG in the absence of supplemental FBS showed that the normalized values of the emission intensities (χ) from the H-like aggregates (at 694-nm spectral peaks) and monomers of ICG (at 791-nm spectral peaks) were comparable at ICG concentrations less than 4 μM [see Fig. 4(a)]. For ICG concentrations ≥ 4 μM, the peak emissions from H-like aggregates were higher than those by the monomer.

In the presence of 5% and 10% FBS, the χ values associated with the monomeric emissions (at 791 nm) were enhanced and became dominant in comparison to those by the H-like aggregates for ICG concentrations in the range of 1.3–19.4 μM [see Fig. 4(b) and (c)]. Similar to the mechanism for enhancement of the monomeric absorbance, we attribute this fluorescence enhancement to the reduced self-aggregation of ICG, which results from binding of 1–2 ICG molecules to the hydrophobic core environment of BSA. Philip *et al.* have reported similar enhancements of the monomeric fluorescence emission of ICG in the presence of HSA [37]. In another study, fluorescence emission of cypate was reported to increase in the presence of BSA [52]. When OrgG, Alexa488, RhodG, and TexRed dyes were dissociated by sodium dodecyl sulfate treatment, monomeric absorbance and fluorescence were enhanced, suggesting that disruption of the aggregate forms of the dyes is a major mechanism to explain the observed enhancements [46].

Corresponding to the enhanced monomeric fluorescence emission of ICG in the presence of FBS, there was an increase in the relative fluorescence quantum yield (ϕ) of ICG in response to 750 nm photoexcitation at a given concentration in the range of 2.6–19.4 μM [see Fig. 5(a)]. Nevertheless, the values of ϕ decreased with increasing ICG concentration regardless of the presence or absence of FBS. This reduction is attributed to the self-quenching of ICG at higher concentrations [34].

We define $\sigma = \phi_{\text{with FBS}}/\phi_{\text{without FBS}}$, where $\phi_{\text{with FBS}}$ and $\phi_{\text{without FBS}}$ correspond to values of ϕ with and without FBS, respectively. Values of σ increased with progressively higher ICG concentrations [see Fig. 5(b)]. For example, there was nearly 3.5-fold increase in σ for 19.4-μM ICG. In absence of FBS, self-aggregation process can be more readily facilitated under high ionic strength (as in the cell culture medium) and with increased ICG concentration. In the presence of FBS, self-aggregation process is hindered since some of ICG molecules can bind to BSA as monomers, thereby reducing the amount of ICG available for self-aggregation.

The levels of FBS utilized in this study were not sufficiently different from each other to induce significant changes in A [see Fig. 1(c) and (d)], χ [see Fig. 4(b) and (c)], ϕ and σ [see Fig. 5(a) and (b)]. In a previous study, when HSA levels were changed by a factor of ≈ 16 from 0.19% to 3%, the monomer absorbance values nearly doubled [51]. To observe such levels of changes in absorbance, in our study, we would have needed to increase FBS levels to as much as 80%, which is not a physiologically relevant value.

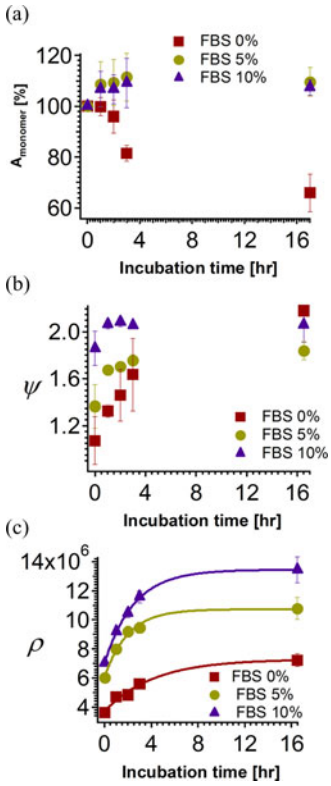

Fig. 6. Effect of incubation time at 37 °C on (a) absorbance values of the ICG monomeric form (A_{monomer}), (b) ratio of monomer to H-like aggregate absorbance (ψ), and (c) normalized integrated fluorescence (ρ). ICG samples (13 μM) were incubated in cell culture medium in dark without and with FBS (5% and 10%). Fluorescence data were obtained in response to photo-excitation at 750 nm. Data points presented in panels (a) and (b) represent average of three measurements at each incubation time, with error bars representing standard deviations. Curves in panel (c) are single exponential fits to the measurements.

We investigated the effect of physiological temperature on absorption and fluorescence properties of ICG in McCoy's 5A cell culture medium with and without supplemental FBS. In the absence of FBS, ICG monomer absorbance decreased by $\approx$ 40% after nearly 17 h of incubation at 37 °C [see Fig. 6(a)]. This decrease in monomer absorbance can be attributed to thermal degradation of ICG with temperature and is consistent with a previous report [54].

In the presence of 5% and 10% FBS, the ICG monomer absorbance actually increased by $\approx$ 7% after 1 h of incubation at 37 °C, and remained at that level for up to nearly 17 h [see Fig. 6(a)]. This increased monomer absorbance with temperature elevation from 25 to 37 °C may be a consequence of conformational changes in BSA, which may result in 1) increased binding affinity to ICG; 2) increased number of BSA binding sites for ICG; and 3) altered hydrophobicity of the local environment that ICG is exposed to. Takeda *et al*. have reported that the proportion of the $\alpha-$helical structure of BSA decreases by $\approx$ 4%, whereas the proportion of the β-structure increases by $\approx$ 50% in response to a temperature change from 25 to 40 °C [55]. Such structural changes of BSA may be sufficient to increase the ICG monomer absorbance as we have observed. Once bound to BSA, the monomer form of ICG remained stable for up to nearly 17 h, hence sustain monomer absorbance over this incubation time interval.

In the absence of FBS, ψ (defined as $A_{\mathrm{monomer}}/A_{\mathrm{H\text{-}like\,aggregate}}$) increased with incubation time of ICG in McCoy's 5a cell culture medium at 37 °C [see Fig. 6(b)]. This result is attributed to progressive reduction in the H-like aggregate absorbance of ICG as compared to that of the monomer with increasing temperature. The reduction in the H-like aggregate absorbance suggests that the aggregate forms of ICG are more susceptible to thermal stress. Other investigators have indicated that aggregate forms of ICG degrade faster than the monomers when ICG is stored at room temperature in dark for 28 days [36]. In the presence of FBS, the values of ψ were greater in comparison with those without FBS for up to 4 h [see Fig. 6(b)]. We attribute this result to higher levels of ICG monomers brought about by BSA binding. By 17 h of incubation, the H-like aggregate form of ICG in the absence of FBS may have been degraded to a sufficiently low level such that the associated value of ψ actually increased and approached to those associated with ICG in the presence of FBS.

In the absence of FBS, the normalized integrated fluorescence (ρ) of ICG in response to photoexcitation at 750 nm increased with incubation time of ICG in McCoy's 5a cell culture medium at 37 °C [see Fig. 6(c)]. This result is a consequence of increased values of ψ with incubation time [see Fig. 6(b)]. In the presence of FBS, the values of ρ were greater in comparison with those without FBS for up to nearly 17 h [see Fig. 6(c)]. We attribute this result to the higher levels of ICG monomers brought about by BSA binding [see Fig. 6(a)], and progressive reduction in the H-like aggregate that does not bind to ICG [see Fig. 6(b)]. Upon binding to BSA, ICG movement is hindered. The restricted molecular vibration and translation of ICG can minimize its conformational distortion and, hence, maintain its absorption and fluorescence properties. However, when ICG is in the cell culture medium without supplemental FBS, temperature elevation readily induces molecular vibrations and translations that lead to changes in the conformation of the dye that ultimately deteriorate its absorption and fluorescence properties [35], [36].

Restricting the molecular translations and vibrations of ICG can help preserve its optical properties from thermal stress. Such restrictions may be achieved by encapsulation of ICG, or binding it to BSA. For example, Rodriguez *et al*. reported that ICG maintained 97% of its original fluorescence emission when it was encapsulated within polymeric micelles formed from poly(styrene-alt-maleic anhydride)-block-poly(styrene) (PSMA-b-PSTY) diblock copolymers at 37 °C for 96 h [56]. In a recent study, Yaseen *et al*. reported that the monomeric absorbance of free ICG decreased by 55% over 48 h of incubation at 40 °C [54]. However, when ICG was encapsulated into constructs composed of poly-allyamine hydrochloride and disodium phosphate with diameters in the range of 400–800 nm, there was only 10% reduction in monomer absorbance under the same conditions.

The enhancement of monomeric absorbance in the presence of albumin [see Fig. 3(a)] has implications in relation to potential phototherapeutic applications of ICG such as photothermal procedures or PDT. Specifically, when using lasers tuned to

the monomeric absorption spectral band of ICG (i.e., $\approx$ 780–800 nm), considerations must be given to the appropriate choice of the radiant exposures given the increased absorbance of ICG monomers. For example, this increased absorbance may allow the use of lower radiant exposures.

The molecular complex consisting of ICG bound to albumin can resemble an optical nanoprobe, which may potentially be used as a contrast agent for accumulation in tumors based on the enhanced permeability and retention (ERP) effect [57]–[59]. Such an effect will be similar to that observed by Maeda and Matsumura where the Evans blue dye, which binds to plasma albumin, selectively accumulated in tumor tissue following intravenous injection [60]. Recently, Kosaka *et al.* demonstrated the feasibility of NIR endoscopic fluorescence imaging of peritoneal ovarian cancer nodules in mice using ICG [61]. Such capability may also be attributed to the accumulation of the ICG-Albumin complex in those tumors due to the EPR effect.

The enhancements in ICG fluorescence emission in the presence of albumin, as evidenced by the increase in its relative fluorescence quantum yield [see Fig. 5(b)], and integrated fluorescence emission at physiological temperature [see Fig. 6(c)], imply that the imaging sensitivity can be increased due to the presence of an ICG-albumin complex. Such an effect is consistent with the use of ICG adsorbed to albumin as a tracer for NIR fluorescence mapping of SLNs in breast cancers and melanomas [62]–[64].

In one study, Hirche *et al.* reported a stronger fluorescent signal associated with use of ICG-HSA complex (5 mg/ml ($\approx$ 6.5 mM) ICG in 20% HSA) as compared to that of 6.5 mM ICG dissolved in 5% glucose solution during lymph node identification in pigs [65], although the differences in signal intensity were not quantified. However, Hutteman *et al.* reported no direct benefit of premixing ICG with HSA prior to injection for SLN mapping in breast cancer patients receiving 500 μM of ICG in distilled water, or 500 μM of ICG-HSA complex in 20% albumin solution [63].

In addition to the differences in the effective concentrations of ICG and ICG-HSA complex upon dilution within the body of pigs versus humans, we offer a further explanation toward the apparent discrepancy between the studies by Hutteman *et al.* [63] and Hirche *et al.* [65]. The effective absorption cross section of ICG in a solution containing albumin [$\sigma^{\mathrm{albumin}}(\lambda)$] can be described as

$$\sigma^{\mathrm{albumin}}(\lambda) = f_M^{\mathrm{albumin}}\sigma_M(\lambda) + f_H^{\mathrm{albumin}}\sigma_H(\lambda) + \sum_{i=1}^{n} f_{M_i}^{*\mathrm{albumin}}\sigma_{M_i}^{*\mathrm{albumin}}(\lambda) \quad (4)$$

where f_M^{albumin} and f_H^{albumin} are the respective fractions of unbound monomeric and H-like aggregate forms of ICG in a given solution containing albumin; $\sigma_m(\lambda)$ is the absorption cross section of unbound ICG monomers; $\sigma_H(\lambda)$ is the absorption cross section of unbound H-like aggregates; $f_{M_i}^{*\mathrm{albumin}}$ is the fraction of ICG monomers bound to albumin with index i representing the number of monomers (i.e., 1, 2) binding to albumin; and $\sigma_{M_i}^{*\mathrm{albumin}}(\lambda)$ is the absorption cross section of bound ICG monomers. Therefore, absorbance of ICG at a given concentration, and subsequently its fluorescence, is related to the presence of various constituent forms consisting of unbound ICG monomers, H-like aggregates, and albumin-bound ICG (either mixed with ICG prior to administration, and/or formed following ICG administration into the body). Nevertheless, our findings reiterate the importance of albumin in enhancing and maintaining the monomeric absorbance at physiological temperature, and increasing the fluorescence quantum yield of ICG.

IV. Conclusion

We investigated the effects of serum at physiologically relevant levels and temperature on absorption and fluorescence characteristics of ICG. Our results indicate that the presence of serum enhances the monomeric absorption of ICG and its fluorescence quantum yield in response to photoexcitation at 750 nm. Presence of serum also preserves the monomeric absorption of ICG and sustains its enhanced fluorescence emission at physiological temperature.

References

[1] J. J. Fox and E. H. Wood, "Application of dilution curves recorded from the right side of the heart or venous circulation with the aid of a new indicator dye," *Proc. Mayo Clin.*, vol. 32, p. 541, 1957.

[2] J. Caesar, S. Sheldon, L. Cianduss, L. Guevara, and S. Sherlock, "The use of indocyanine green in the measurement of hepatic blood flow and as a test for hepatic function," *Clin. Sci.*, vol. 21, pp. 43–57, 1961.

[3] J. V. Frangioni, "In vivo near-infrared fluorescence imaging," *Curr. Opin. Chem. Biol.*, vol. 7, pp. 626–634, 2003.

[4] L. A. Yannuzzi, "Indocyanine green angiography: A perspective on use in the clinical setting," *Amer. J. Ophthalmol.*, vol. 151, pp. 745–751, 2011.

[5] H. Nimura, N. Narimiya, N. Mitsumori, Y. Yamazaki, K. Yanaga, and M. Urashima, "Infrared ray electronic endoscopy combined with indocyanine green injection for detection of sentinel nodes of patients with gastric cancer," *Brit. J. Surg.*, vol. 91, pp. 575–579, 2004.

[6] T. Kitai, T. Inomoto, M. Miwi, and T. Shikayama, "Fluorescence navigation with indocyanine green for detecting sentinel lymph nodes in breast cancer," *Breast Cancer*, vol. 12, pp. 211–215, 2005.

[7] E. M. Sevick-Muraca, R. Sharma, J. C. Rasmussen, M. V. Marshall, J. A. Wendt, H. Q. Pham, E. Bonefas, J. P. Houston, L. Sampath, K. E. Adams, D. K. Blanchard, R. E. Fisher, S. B. Chiang, R. Elledge, and M. E. Mawad, "Imaging of lymph flow in breast cancer patients after microdose administration of a near-infrared fluorophore: Feasibility study," *Radiology*, vol. 246, pp. 731–741, 2008.

[8] I. Miyashiro, N. Miyoshi, M. Hiratsuka, K. Kishi, T. Yamada, M. Ohue, H. Ohigashi, M. Yano, O. Ishikawa, and S. Imaoka, "Detection of sentinel node in gastric cancer surgery by indocyanine green fluorescence imaging: Comparison with infrared imaging," *Ann. Surg. Oncol.*, vol. 15, pp. 1640–1643, 2008.

[9] C. Hirche, D. Murawa, Z. Mohr, S. Kneif, and M. Hunerbein, "ICG fluorescence-guided sentinel lymph node biopsy for axillary nodal staging in breast cancer," *Breast Cancer Res. Treat.*, vol. 121, pp. 373–378, 2010.

[10] A. Hirano, M. Kamimura, K. Ogura, N. Kim, A. Hattori, Y. Setoguchi, F. Okubo, H. Inoue, R. Miyamoto, J. Kinoshita, M. Fujibayashi, and T. Shimizu, "A comparison of indocyanine green fluorescence imaging plus blue dye and blue dye alone for sentinel node navigation surgery in breast cancer patients," *Ann. Surg. Oncol.*, vol. 19, pp. 4112–4116, 2012.

[11] H. Uhara, N. Yamazaki, M. Takata, A. Sakakibara, Y. Nakamura, K. Suehiro, A. Yamamoto, R. Kamo, K. Mochida, H. Takenaka, T. Yamashita, T. Takenouchi, S. Yoshikawa, A. Takahashi, J. Uehara, M. Kawai, H. Iwata, T. Kanodo, Y. Kai, S. Wantabe, S. Murata, T. Ikeda, H. Fukamizu, T. Tanaka, N. Hatta, and T. Saida, "Applicability of radiocolloids, blue dyes and fluorescent indocyanine green to sentinel node biopsy in melanoma," *J. Dermatol.*, vol. 39, pp. 336–338, 2012.

[12] J. R. van der Vorst, B. E. Schaafsma, F. P. Verbeek, R.J. Swijnenburg, M. Hutteman, G. J. Liefers, C. J. van de Velde, J. V. Frangioni, and A. L. Vahrmeijer, "Dose optimization for near-infrared fluorescence sentinel

lymph node mapping in patients with melanoma," *Brit. J. Dermatol.*, vol. 168, pp. 93–98, 2013.

[13] C. Hirche, H. Engel, Z. Hirche, S. Doniga, T. Herold, U. Kneser, M. Lenhardt, and M. Hunerbein, "Real-time lymphography by indocyanine green fluorescence: Improved navigation for regional lymph node staging," *Ann. Plast. Surg.*, 2013. Available: http://journals.lww.com/annalsplasticsurgery/pages/articleviewer.aspx?year=9000&issue=00000&article=98857&type=abstract.

[14] T. Yamamoto, M. Narushima, K. Doi, A. Oshima, F. Ogata, M. Mihara, I. Koshima, and G. Mundinger, "Characteristic indocyanine green lymphography findings in lower extremity lymphedema: The Generation of a novel lymphedema severity staging system using dermal backflow patterns," *Plast. Reconstr. Surg.*, vol. 127, pp. 1979–1986, 2011.

[15] T. Yamamoto, N. Yamamoto, K. Doi, A. Oshima, H. Yoshimatsu, T. Todokoro, F. Ogata, M. Mihara, M. Narushima, T. Lida, and I. Koshima, "Indocyanine green-enhanced lymphography for upper extremity lymphedema: A novel severity staging system using dermal backflow patterns," *Plast. Reconstr. Surg.*, vol. 128, pp. 491–947, 2011.

[16] M. Mihara, H. Hara, Y. Hayashi, T. Lida, J. Araki, A. Yamamoto, T. Todokoro, M. Narushima, N. Murai, and I. Koshima, "Upper-limb lymphedema treated aesthetically with lymphaticovenous anastomosis using indocyanine green lymphography and noncontact vein visualization," *J. Reconstr. Microsurg.*, vol. 28, pp. 327–332, 2012.

[17] H. Hara, M. Mihara, A. Hayashi, M. Kanemaru, T. Todokoro, A. Yamamoto, T. Lida, R. Hino, and I. Koshima, "Therapeutic strategy for lower limb lymphedema and lymphatic fistula after resection of a malignant tumor in the hip joint region: A case report," *Microsurgery*, 2013. Available: http://onlinelibrary.wiley.com/doi/10.1002/micr.22138/abstract;jsessionid=A7ACB35B2876407A2E8FC3520FE58307.d04t03.

[18] M. Mihara, H. Hara, J. Araki, M. Narushima, L. Lida, and I. Koshima, "Treatment of hand lymphedema with free flap transfer and lymphangiogenesis analysis after hand retention using indocyanine green (ICG) lymphography and histological analysis," *J. Plast. Reconstr. Aesthet. Surg.*, 2013. Available: http://www.jprasurg.com/article/S1748-6815(13)00406-3/abstract.

[19] D. A. Sherwinter, J. Gallagher, and T. Donkar, "Intra-operative transanal near infrared imaging of colorectal anastomotic perfusion: A feasibility study," *Colorectal Dis.*, vol. 15, pp. 91–96, 2013.

[20] M. D. Jafari, K. H. Lee, W. J. Halabi, S. D. Mills, J. C. Carmichael, M. J. Stamos, and A. Pigazzi, "The use of indocyanine green fluorescence to assess anastomotic perfusion during robotic assisted laparoscopic rectal surgery," *Surg. Endosc.*, vol. 27, pp. 3003–3008, 2013.

[21] K. Polom, D. Murawa, Y. S. Rho, P. Nowaczyk, M. Hunerbein, and P. Murawa, "Current trends and emerging future of indocyanine green usage in surgery and oncology," *Cancer*, vol. 117, pp. 4812–4822, 2011.

[22] C. Abels, "Targeting of the vascular system of solid tumours by photodynamic therapy (PDT)," *Photochem. Photobiol. Sci.*, vol. 3, pp. 765–771, 2004.

[23] T. Funayama, M. Sakane, T. Abe, and N. Ochiai, "Photodynamic therapy with indocyanine green injection and near-infrared light irradiation has phototoxic effects and delays paralysis in spinal metastasis," *Photomed. Laser Surg.*, vol. 30, pp. 47–53, 2012.

[24] E. Smretschnig, S. Ansari-Shahrezaei, S. Hagen, G. Glittenberg, I. Krebs, and S. Binder, "Half-fluence photodynamic therapy in chronic central serous chorioretinopathy," *Retina*, vol. 33, pp. 316–323, 2013.

[25] L. S. Bass, N. Moazami, J. Pocsidio, M. C. Oz, P. Logerfo, and M. R. Treat, "Changes in type-I collagen following laser-welding," *Laser Surg. Med.*, vol. 12, pp. 500–505, 1992.

[26] V. V. Tuchin, E. A. Genina, A. N. Bashkatov, G. V. Simonenko, O. D. Odoevskaya, and G. B. Altshuler, "A pilot study of ICG laser therapy of acne vulgaris: Photodynamic and photothermolysis treatment," *Lasers Surg. Med.*, vol. 33, pp. 296–310, 2003.

[27] A. Klein, R. M. Szeimies, W. Baumler, F. Zeman, S. Schreml, U. Hohenleutner, M. Landthaler, M. Koller, and P. Babilas, "Indocyanine green-augmented diode laser treatment of port-wine stains: Clinical and histological evidence for a new treatment option from a randomized controlled trial," *Brit. J. Dermatol.*, vol. 167, pp. 333–342, 2012.

[28] G. R. Cherrick, S. W. Stein, C. M. Leevy, and C. S. Davidson, "Indocyanine green: Observations on its physical properties, plasma decay, and hepatic extraction," *J. Clin. Invest.*, vol. 39, pp. 592–600, 1960.

[29] K. J. Baker, "Binding of sulfobromophthalein (BSP) sodium and indocyanine green (ICG) by plasma alpha1 lipoproteins," *Proc. Soc. Exp. Biol. Med.*, vol. 122, pp. 957–963, 1966.

[30] T. J. Muckle, "Plasma-proteins binding of indocyanine green," *Biochem. Med.*, vol. 15, pp. 17–21, 1976.

[31] R. C. Benson and H. A. Kues, "Fluorescence properties of indocyanine green as related to angiography," *Phys. Med. Biol.*, vol. 23, pp. 159–163, 1978.

[32] S. Mordon, J. M. Devoisselle, S. Soulie-Begu, and T. Desmettre, "Indocyanine green: Physicochemical factors affecting its fluorescence in vivo," *Microvasc. Res.*, vol. 55, pp. 146–152, 1998.

[33] S. Yoneya, T. Saito, Y. Komatsu, I. Koyama, t. Takahashi, and J. Duvoll-Young, "Binding properties of indocyanine green in human blood," *Invest. Ophthalmol. Vis. Sci.*, vol. 39, pp. 1286–1290, 1998.

[34] T. Desmettre, J. M. Devoisselle, and S. Mordon, "Fluorescence properties and metabolic features of indocyanine green (ICG) as related to angiography," *Survey Ophthalmol.*, vol. 45, pp. 15–27, 2000.

[35] J. Gathje, R. R. Steuer, and K. R. Nicholes, "Stability studies on indocyanine green dye," *J. Appl. Physiol.*, vol. 29, pp. 181–185, 1970.

[36] W. Holzer, M. Mauerer, A. Penzkofer, R. M. Szeimies, C. Abels, M. Landthaler, and W. Baumler, "Photostability and thermal stability of indocyanine green," *J. Photochem. Photobiol. B.*, vol. 47, pp. 155–164, 1998.

[37] R. Philip, A. Penzkofer, W. Baumler, R. M. Szeimies, and C. Abels, "Absorption and fluorescence spectroscopic investigation of indocyanine green," *J. Photochem. Photobiol. A*, vol. 96, pp. 137–148, 1996.

[38] T. L. Testerman, D. J. McGee, and H. L. T. Mobley, "Helicobacter pylori growth and urease detection in the chemically defined medium Ham's F-12 nutrient mixture," *J. Clin. Microbiol.*, vol. 39, pp. 3842–3850, 2001.

[39] F. Bertolero, M. E. Kaighn, R. F. Camalier, and U. Saffiotti, "Effects of serum and serum-derived factors on growth and differentiation of mouse keratinocytes," *In Vitro Cell. Dev. Biol.*, vol. 22, pp. 423–428, Jul. 1986.

[40] X. Y. Zheng, H. Baker, W. S. Hancock, F. Fawaz, M. McCaman, and E. Pungor, "Proteomic analysis for the assessment of different lots of fetal bovine serum as a raw material for cell culture. Part IV. Application of proteomics to the manufacture of biological drugs," *Biotechnol. Prog.*, vol. 22, pp. 1294–1300, 2006.

[41] M. Mauerer, A. Penzkofer, and J. Zweck, "Dimerization, J-aggregation and J-disaggregation dynamics of indocyanine green in heavy water," *J. Photochem. Photobiol. B*, vol. 47, pp. 68–73, 1998.

[42] M. L. J. Landsman, G. Kwant, G. A. Mook, and W. G. Zijlstra, "Light-absorbing properties, stability, and spectral stabilization of indocyanine green," *J. Appl. Physiol.*, vol. 40, pp. 575–583, 1976.

[43] A. H. Herz, "Aggregation of sensitizing dyes in solution and their adsorption onto silver-halides," *Adv. Colloid Interface Sci.*, vol. 8, pp. 237–298, 1977.

[44] M. Kasha, H. R. Rawls, and M. Ashraf El-Bayoumi, "The exciton model in molecular spectroscopy," *Pure Appl. Chem.*, vol. 11, pp. 371–392, 1965.

[45] O. Valdesaguilera and D. C. Neckers, "Aggregation phenomena in xanthene dyes," *Accounts Chem. Res.*, vol. 22, pp. 171–177, 1989.

[46] M. Ogawa, N. Kosaka, P. L. Choyke, and H. Kobayashi, "H-type dimer formation of fluorophores: A mechanism for activatable, in vivo optical molecular imaging," *ACS Chem. Biol.*, vol. 4, pp. 535–546, 2009.

[47] G. Patonay, J. S. Kim, R. Kodagahally, and L. Strekowski, "Spectroscopic study of a novel bis(heptamethine cyanine) dye and its interaction with human serum albumin," *Appl. Spectrosc.*, vol. 59, pp. 682–690, 2005.

[48] G. Beckford, E. Owens, M. Henary, and G. Patonay, "The solvatochromic effects of side chain substitution on the binding interaction of novel tricarbocyanine dyes with human serum albumin," *Talanta*, vol. 92, pp. 45–52, 2012.

[49] J. Steinhardt, J. Krijn, and J. G. Leidy, "Differences between bovine and human Serum albumins: Binding isotherms, optical rotatory dispersion, viscosity, hydrogen ion titration, and fluorescence effects," *Biochemistry*, vol. 10, pp. 4005–4015, 1971.

[50] E. L. Gelamo and M. Tabak, "Spectroscopic studies on the interaction of bovine (BSA) and human (HSA) serum albumins with ionic surfactants," *Spectrochimca Acta A*, vol. 56, pp. 2255–2271, 2000.

[51] J. F. Zhou, M. P. Chin, and S. A. Schafer, "Aggregation and degradation of indocyanine green," in *SPIE Proc.*, Bellingham, CA, USA, 1994, pp. 495–505.

[52] M. Y. Berezin, H. Lee, W. Akers, G. Nikiforovich, and S. Achilefu, "Ratiometric analysis of fluorescence lifetime for probing binding sites in albumin with near-infrared fluorescent molecular probes," *Photochem. Photobiol.*, vol. 83, pp. 1371–1378, 2007.

[53] M. Kiselev and D. Ivlev, "The study of hydrophobicity in water-methanol and water-tert-butanol mixtures," *J. Mol. Liq.*, vol. 110, pp. 193–199, 2004.

[54] M. A. Yaseen, J. Yu, M. S. Wong, and B. Anvari, "Stability assessment of indocyanine green within dextran-coated mesocapsules by absorbance spectroscopy," *J. Biomed. Opt.*, vol. 12, p. 064031, 2007.

[55] K. Takeda, A. Wada, K. Yamamoto, Y. Moriyama, and K. Aoki, "Conformational change of bovine serum-albumin by heat-treatment," *J. Protein Chem.*, vol. 8, pp. 653–659, Oct. 1989.
[56] V. B. Rodriguez, S. M. Henry, A. S. Hoffman, P. S. Stayton, X. D. Li, and S. H. Pun, "Encapsulation and stabilization of indocyanine green within poly(styrene-alt-maleic anhydride) block-poly(styrene) micelles for near-infrared imaging," *J. Biomed. Opt.*, vol. 13, p. 0140025, 2008.
[57] Y. Matsumura and H. Maeda, "A new concept for macromolecular therapeutics in cancer chemotherapy: Mechanism of tumoritropic accumulation of proteins and the antitumor agent smancs," *Cancer Res.*, vol. 46, pp. 6387–6392, 1986.
[58] H. Maeda and Y. Matsumura, "EPR effect based drug design and clinical outlook for enhanced cancer chemotherapy," *Adv. Drug Del. Rev.*, vol. 18, pp. 129–130, 2011.
[59] V. Torchilin, "Tumor delivery of macromolecular drugs based on the EPR effect," *Adv. Drug Del. Rev.*, vol. 63, pp. 131–135, 2011.
[60] H. Maeda and Y. Matsumura, "Cancer selective macromolecular therapeutics: Tailoring of an antitumor protein drug," in *Protein Tailoring for Food and Medical Uses*, R. E. Freeney and J. R. Whitaker, Eds. New York, NY, USA: Marcel Dekker, 1986, pp. 353–382.
[61] N. Kosaka, M. Mitsunaga, M. R. Longmire, P. L. Choyke, and H. Kobayashi, "Near infrared fluorescence-guided real-time endoscopic detection of peritoneal ovarian cancer nodules using intravenously injected indocyanine green," *Int. J. Cancer*, vol. 29, pp. 1671–1677, 2011.
[62] S. L. Troyan, V. Kianzad, S. L. Gibbs-Strauss, S. Gioux, A. Matsui, R. Oketokoun, L. Ngo, A. Khamene, F. Azar, and J. V. Frangioni, "The flare intraoperative near-infrared fluorescence imaging system: A first-in-human clinical trial in breast cancer sentinel lymph node mapping," *Ann. Surg. Oncol.*, vol. 16, pp. 2943–2952, 2009.
[63] M. Hutteman, J. S. D. Mieog, J. R. van der Vorst, G. L. Liefers, H. Putter, C. W. G. M. Lowik, J. V. Frangioni, C. J. H. van de Velde, and A. L. Vahrmeijer, "Randomized, double-blind comparison of indocyanine green with or without albumin premixing for near-infrared fluorescence imaging of sentinel lymph nodes in breast cancer patients," *Breast Cancer Res. Treat.*, vol. 127, pp. 163–170, 2011.
[64] K. Polom, D. Murawa, Y. S. Rho, A. Spychala, and P. Murawa, "Skin melanoma sentinel lymph node biopsy using real-time fluorescence navigation with indocyanine green and indocyanine green with human serum albumin," *Brit. J. Dermatol.*, vol. 166, pp. 682–683, 2012.
[65] C. Hirche, H. Engel, L. Kolios, J. Cognie, M. Hunerbein, M. Lenhardt, and T. Kremer, "An experimental study to evaluate the fluobeam 800 imaging system for fluorescence-guided lymphatic imaging and sentinel node biopsy," *Surg. Innov.*, 2012. Available: http://sri.sagepub.com/content/early/2012/12/27/1553350612468962.full.pdf.

Bongsu Jung received the B.S. degree in biomedical engineering from Yonsei University, Seoul, Korea, and worked as a Hardware Research Engineer in ultrasound diagnostic systems R&D center, General Electric Healthcare, Korea. Subsequently, he received the Ph.D. degree in biomedical engineering from The University of Texas at Austin. He was a Research Scientist in the Department of Bioengineering at University of California, Riverside, CA, USA, and joined Daegu-Gyeongbuk Medical Innovation Foundation in Korea in 2013 as a Principal Research Scientist of the Medical Device Development Center. His scientific interests include biophotonics, multifunctional nanoparticles, surface Plasmon resonance, near infrared imaging, and cancer theranostics.

Valentine I. Vullev received the B.S. degree in chemistry and physics from Keene State College, St. Keene, NH, USA, and the Ph.D. degree in chemistry from Boston University, Boston, MA, USA, where his research was in the area of photochemistry and biophysics. As a Postdoctoral Fellow at Harvard University, his research expanded into the areas of surface chemistry and microfluidics. He is currently an Associate Professor in bioengineering, chemistry, biochemistry, and materials science and engineering at the University of California, Riverside, CA, USA. His current areas of research encompass photoinduced charge transfer in engineered bioinspired electrets, optomicrofluidics, photoactive and bioactive interfaces, and photophysics of organic agents for imaging and other biomedical applications.

Bahman Anvari received the B.S. degree in biophysics from the University of California, Berkeley, CA, USA, and Ph.D. degree in bioengineering from Texas A&M University, College Station, TX, USA. He was a Postdoctoral Fellow at Beckman Laser Institute and Medical Clinic, University of California, Irvine, CA, USA, and later a Research Assistant Professor at Harvey Mudd College, Claremont, CA. He joined the Department of Bioengineering at Rice University in 1998 as an Assistant Professor, and became an Associate Professor in 2003. He joined the Department of Bioengineering, University of California, as a Professor in 2006. His research interests in biophotonics include the engineering and applications of nanostructured materials for phototheranostic applications, and use of optical methods including laser tweezers in studying cell mechanics. He is a Fellow of the American Institute for Medical and Biological Engineering and the American Association for the Advancement of Science.